

Observation of Rydberg Blockade Due to the Charge-Dipole Interaction between an Atom and a Polar Molecule

Alexander Guttridge^{1,2}, Daniel K. Ruttley^{1,2}, Archie C. Baldock¹, Rosario González-Férez³,
H. R. Sadeghpour⁴, C. S. Adams^{1,2,*} and Simon L. Cornish^{1,2,†}

¹*Department of Physics, Durham University, South Road, Durham, DH1 3LE, United Kingdom*

²*Joint Quantum Centre Durham-Newcastle, Durham University, South Road, Durham, DH1 3LE, United Kingdom*

³*Instituto Carlos I de Física Teórica y Computacional, and Departamento de Física Atómica, Molecular y Nuclear, Universidad de Granada, 18071 Granada, Spain*

⁴*ITAMP, Center for Astrophysics | Harvard & Smithsonian, Cambridge, Massachusetts 02138, USA*



(Received 10 March 2023; accepted 15 May 2023; published 7 July 2023)

We demonstrate Rydberg blockade due to the charge-dipole interaction between a single Rb atom and a single RbCs molecule confined in optical tweezers. The molecule is formed by magnetoassociation of a Rb + Cs atom pair and subsequently transferred to the rovibrational ground state with an efficiency of 91(1)%. Species-specific tweezers are used to control the separation between the atom and molecule. The charge-dipole interaction causes blockade of the transition to the Rb(52s) Rydberg state, when the atom-molecule separation is set to 310(40) nm. The observed excitation dynamics are in good agreement with simulations using calculated interaction potentials. Our results open up the prospect of a hybrid platform where quantum information is transferred between individually trapped molecules using Rydberg atoms.

DOI: 10.1103/PhysRevLett.131.013401

Ultracold dipolar systems, such as Rydberg atoms and polar molecules, are promising platforms for quantum simulation and computation [1–14]. Rydberg atoms exhibit strong, long-range interactions that can be exploited to engineer quantum entanglement and multiqubit gates [12,15–20]. This approach exploits the Rydberg blockade mechanism, where strong van der Waals interactions between neighboring Rydberg atoms prevent simultaneous excitation of multiple atoms within a certain radius. Ultracold polar molecules also exhibit long-range interactions and possess a rich manifold of long-lived rotational states which can be coupled using microwave fields [21–23] to realize high-fidelity quantum operations [24–29]. Recent advances in optical tweezer arrays of Rydberg atoms [10–13] and ultracold molecules [30–35] provide the foundation to develop hybrid atom-molecule systems.

A hybrid system composed of polar molecules and Rydberg atoms trapped in optical tweezer arrays offers a way to combine the advantages of both platforms. For example, quantum information can be encoded in the internal states of the molecule, and gates can be performed utilizing the strong interactions of Rydberg atoms [36–39]. This combines the fast high-fidelity interactions and readout possible with Rydberg atoms [20,40] with the long

coherence times and lifetimes of polar molecules [21–23]. In addition, this hybrid system offers new capabilities, such as nondestructive readout of the molecular state [41–43], cooling of molecules using Rydberg atoms [44,45], and photoassociation of giant polyatomic Rydberg molecules [46–48].

Realizing controlled interactions between molecules and Rydberg atoms remains an outstanding challenge. These interactions extend beyond the van der Waals and dipole-dipole interactions which have been widely used in single-species Rydberg systems [11] and the dipole-dipole interactions recently observed between polar molecules [49–52]. The long-range interaction of the Rydberg electron with the permanent dipole, \mathbf{d} , of the polar molecule takes, in first order, the form of a charge-dipole interaction [46,53]. The interaction arises when the internal field due to the Rydberg electron and atomic core polarizes the molecular dipole, $V_{cd}(\mathbf{r}, \mathbf{R}_{am}) = BN^2 - \mathbf{d} \cdot \mathbf{F}(\mathbf{r}, \mathbf{R}_{am})$. Here \mathbf{r} is the electron position, \mathbf{R}_{am} is the dipole position with respect to the atomic core, and \mathbf{N} and B are the quantum operators for molecular rotation and the associated rotational constant, respectively. The internal electric field is $\mathbf{F} = e(\mathbf{r} - \mathbf{R}_{am})/|\mathbf{r} - \mathbf{R}_{am}|^3 + e\mathbf{R}_{am}/R_{am}^3$, leading to an anisotropic $1/R_{am}^2$ interaction. For micron-scale separations, achievable in optical lattices and optical tweezers, these interactions are predicted to be strong enough to preclude the excitation of an atom to a Rydberg state in the presence of a molecule [36,37].

In this Letter, we demonstrate Rydberg blockade due to the charge-dipole interaction in a hybrid platform

Published by the American Physical Society under the terms of the Creative Commons Attribution 4.0 International license. Further distribution of this work must maintain attribution to the author(s) and the published article's title, journal citation, and DOI.

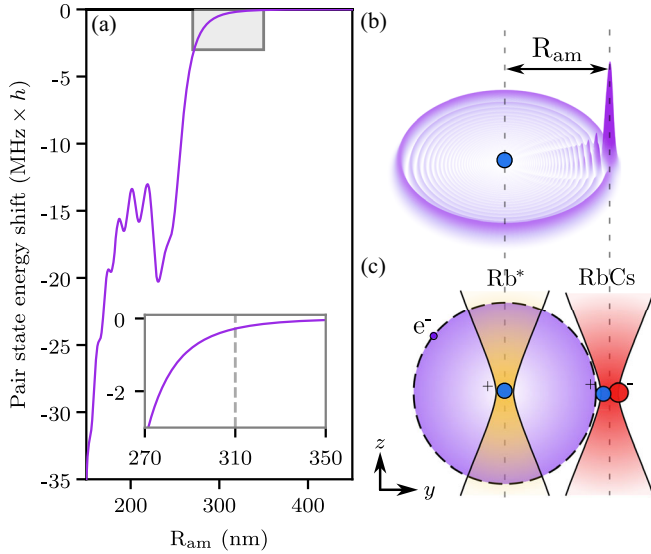


FIG. 1. (a) Pair state energy shift as a function of the separation R_{am} between a Rb atom in state $|r\rangle = |52s\rangle$ and a RbCs molecule in state $|G\rangle = |X^1\Sigma^+, v=0, N=0\rangle$. The shaded region (shown inset) highlights the region relevant to the blockade measurements; the dashed line shows our best estimate of R_{am} and the range reflects the associated uncertainty. (b) A surface plot of the radial electron density of the Rydberg electron for $R_{\text{am}} = 230$ nm. (c) Schematic of the experiment showing the atom and molecule trapped in species-specific optical tweezers separated along the y axis.

composed of a single ^{87}Rb atom and a single $^{87}\text{Rb}^{133}\text{Cs}$ molecule confined in separate optical tweezers. The molecule is prepared in the rovibrational ground state using a combination of magnetoassociation and coherent optical transfer. We use species-specific optical tweezers to control the atom-molecule separation down to ~ 300 nm without significant collisional loss. At this separation, we find that excitation of the Rb atom to a Rydberg state is suppressed.

The adiabatic Hamiltonian for the hybrid Rydberg atom-molecule system at large separations contains the charge induced-dipole interaction [46], and the S -wave scattering of the slow electron from the molecule [53–55]. The results described here hold for $d < d_{\text{cr}} = 1.639$ Debye [67], the Fermi-Teller critical dipole, to ensure that the electron only scatters from the molecule. The trapping potentials due to the optical tweezers and the effect of the magnetic field are neglected in the theoretical description.

In Fig. 1(a), we show the resulting energy shift as a function of the separation R_{am} between a Rb atom in Rydberg state $|r\rangle = |52s\rangle$ and a RbCs molecule in the rovibrational ground state $|G\rangle = |X^1\Sigma^+, v=0, N=0\rangle$ with $d = 1.225$ Debye [68] and $B = 0.490$ GHz [69]. Here, v and N are the vibrational and rotational quantum numbers, respectively. At $R_{\text{am}} \sim 300$ nm, we see the onset of a large shift arising from the charge-dipole interaction. The modulation in the energy arise from the oscillatory nature of the Rydberg electron wave function. For our

choice of states the interaction is nonresonant and van der Waals interactions are ≈ 1 kHz at these distances. Figure 1(b) shows the Rydberg electron density for our system with $R_{\text{am}} = 230$ nm, highlighting the perturbation due to the polar molecule. The outermost minimum of the Rydberg electron wave function sets the range of interactions; this occurs at 220 nm for the state $|r\rangle$.

The experimental geometry is shown in Fig. 1(c). The atom and molecule are prepared in species-specific tweezers. Both particles predominantly occupy the motional ground state of their respective traps. The tweezer separation, R_t , is set by controlling the relative tweezer alignment in all three spatial dimensions. The atom-molecule separation, R_{am} , is determined from the difference in the resulting potential minima. When the tweezers overlap, the atom-molecule separation is reduced compared to the tweezer separation ($R_{\text{am}} < R_t$) due to the effect of each potential on the other species. For each measurement, we repeat an experimental sequence many times. Fluctuations in the relative alignment of the tweezers occur from shot to shot with an estimated standard deviation of 50 nm in each coordinate. Atomic fluorescence images are taken at the start and end of each sequence to determine the occupancy of each tweezer; molecules are detected by reversing the association procedure and imaging the resulting atom pair in separate tweezers. We apply various postselection criteria on the tweezer occupancies to obtain values and their associated confidence intervals from typically 200–1000 runs for different experimental scenarios [55].

Our experiments begin by loading single ^{87}Rb and ^{133}Cs atoms into species-specific optical tweezers [70]. After determining the trap occupations and performing rearrangement, the atoms are further cooled using Raman sideband cooling [71–73] and transferred to the hyperfine states $|f=1, m_f=1\rangle_{\text{Rb}} + |f=3, m_f=3\rangle_{\text{Cs}}$. To produce a molecule, we must prepare a Rb + Cs atom pair in the ground state of relative motion in a single tweezer. We achieve this by merging a 817 nm tweezer containing a Rb atom into a 1065 nm tweezer containing a Cs atom. This protocol prepares a Rb + Cs atom pair in the ground state of relative motion in 56(5)% of runs [73].

The electronic potential energy curves for RbCs are shown in Fig. 2(a). Weakly bound RbCs molecules in state $|F\rangle$ are formed using magnetoassociation on an interspecies Feshbach resonance at 197 G [35,74–76]. The magnetic field ramps used to associate and later dissociate the atom pair are shown in the upper panel of Fig. 2(b); the central panel shows the energy levels that these ramps navigate to access the state $|F\rangle$ at 181.6 G. The formation of weakly bound RbCs molecules is detected using pump-induced loss [55,77–79] which precludes atom-pair recovery when the association and merging steps are reversed [Fig. 2(b) lower panel].

We transfer the weakly bound molecule to the rovibrational ground state $|G\rangle$ using two-photon stimulated Raman

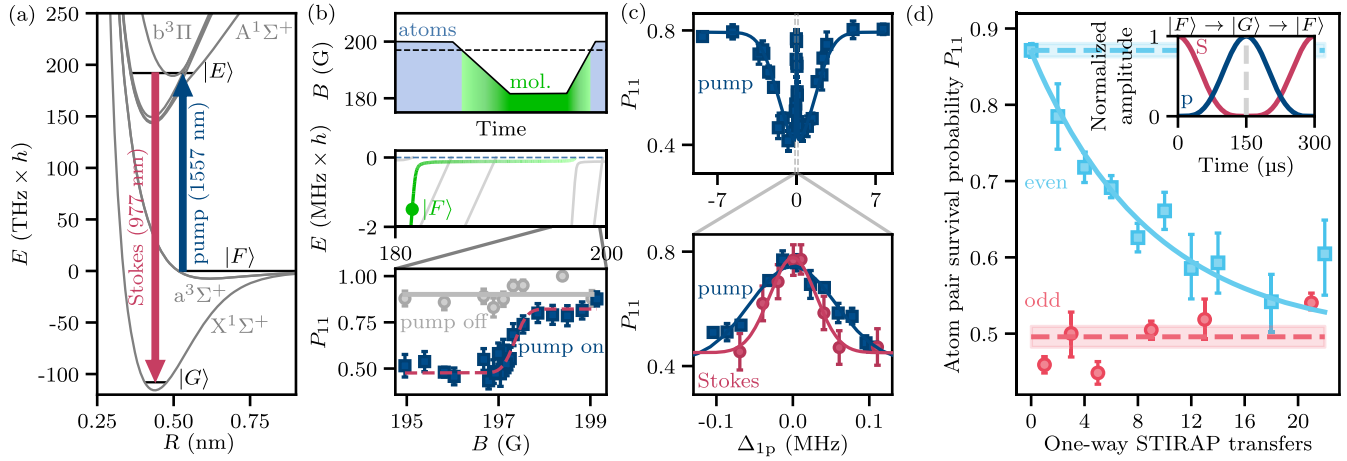


FIG. 2. Formation of ground state RbCs molecules in optical tweezers. (a) Electronic potential curves for RbCs showing the pump and Stokes transitions that couple states $|F\rangle$, $|E\rangle$, and $|G\rangle$. (b) Formation of weakly bound molecules by magnetoassociation of atom pairs using a Feshbach resonance at 197 G. The top panel shows the magnetic field ramps used to form molecules and then navigate the near-threshold bound states shown in the middle panel. STIRAP is performed at 181.6 G when the molecule occupies the state $|F\rangle$ (indicated point). The lower panel shows the pump-induced loss of weakly bound molecules. The atom-pair survival probability P_{11} is measured after reversing the field ramp to dissociate any remaining molecules. (c) Atom-pair survival probability for a round trip $|F\rangle \rightarrow |G\rangle \rightarrow |F\rangle$ as a function of the one-photon detuning Δ_{1p} of either the pump (from the transition $|F\rangle \rightarrow |E\rangle$) or the Stokes (from the transition $|E\rangle \rightarrow |G\rangle$) when the other laser is on resonance. (d) Repeated STIRAP transfers between states $|F\rangle$ and $|G\rangle$ with a one-way efficiency of 91(1)%. The dashed lines show the experimental contrast; the shaded regions are the uncertainties. The inset shows the pulse profiles for a round-trip transfer.

adiabatic passage (STIRAP) [80,81], as previously demonstrated for bulk gases of RbCs molecules [68,77,79,82]. In Fig. 2(c) we show the probability of recovering the atom pair after a round trip $|F\rangle \rightarrow |G\rangle \rightarrow |F\rangle$ as a function of the single-photon detuning of either the pump or Stokes lasers, with the other laser held on single-photon resonance. When the Stokes laser is not resonant, the pump laser causes loss to other molecular states via the intermediate molecular state $|E\rangle = |^3\Pi_1, v' = 29, J' = 1\rangle$. When the pump laser is far from resonant, the molecules remain in state $|F\rangle$ throughout the transfer sequence.

In Fig. 2(d), we characterize the STIRAP efficiency using repeated transfers back and forth between states $|F\rangle$ and $|G\rangle$. An odd number of successful one-way transfers results in the molecule occupying state $|G\rangle$, whereas an even number returns it to state $|F\rangle$. Only molecules that occupy state $|F\rangle$ at the end of the sequence are dissociated back into atom pairs for detection. The offset of the odd points indicates the combined efficiency of the cooling, merging, and magnetoassociation stages; in 50(1)% of runs we do not form a molecule, and thus reimage the atom pair independent of the STIRAP pulses. The maximum contrast between the odd and even points is limited primarily by the 35(5) ms lifetime of molecules in state $|F\rangle$ in the trap and the need to allow the magnetic field to stabilize before STIRAP [55]. We measure a one-way transfer efficiency of 91(1)%, consistent with the best reported efficiencies for RbCs in bulk gases [79,82].

To observe blockade, the charge-dipole interaction between the Rydberg atom and the molecule must be

greater than the power-broadened transition linewidth. For our system, this is set by the Rabi frequency of 500(3) kHz; blockade therefore requires interactions shifts $\gtrsim 1$ MHz. Our calculations in Fig. 1 predict the atom-molecule distance must be below a blockade radius ~ 300 nm to observe this effect, a distance smaller than the beam radii of the individual tweezers (~ 1 μm). We cannot achieve submicron separations by loading both species into the same tweezer, as the expected lifetime due to collisional loss is < 1 ms [83]. Instead we utilize species-specific tweezers at wavelengths of 1065 nm for the molecule and 817 nm for the atom. For the Rb atom, the ratio of polarizabilities for these wavelengths is $\alpha_{817}^{\text{Rb}}/\alpha_{1065}^{\text{Rb}} \sim 6.3$ [84], so that it is confined predominantly in the 817 nm tweezer (the ‘‘atom tweezer’’). Conversely, for the RbCs molecule $\alpha_{1065}^{\text{RbCs}}/\alpha_{817}^{\text{RbCs}} \sim 4.5$ [85] so that it is confined predominantly in the 1065 nm tweezer (the ‘‘molecule tweezer’’). Typical trap potentials are illustrated in the insets of Fig. 3.

We investigate loss due to collisions between a Rb atom in state $|g\rangle = |5s_{1/2}, f = 1, m_f = 1\rangle$ and a RbCs molecule by sweeping the position of the atom tweezer to a variable distance R_t from the molecule tweezer. The particles are held at this separation for 9.5 ms before the sweep is reversed and the particle survival probabilities are measured. The results are presented in Fig. 3. For the molecule, we report the atom-pair survival probability, postselected on cases where a weakly bound molecule was formed [55]. The upper panel shows the one-body survival probabilities from runs where *either* the Rb atom *or* the RbCs molecule

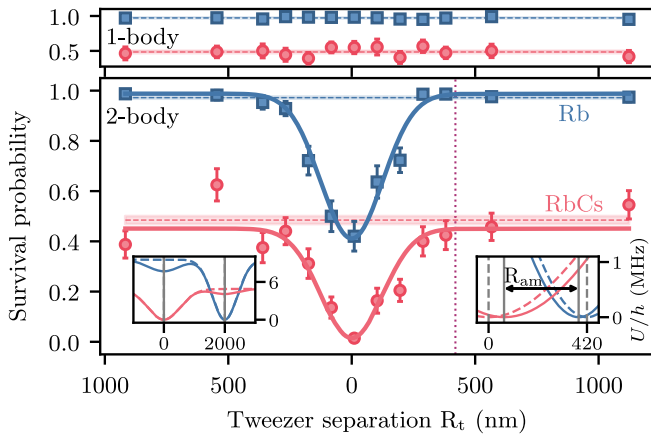


FIG. 3. Collisions between ground state RbCs molecules and Rb atoms held in separate species-specific optical tweezers. Particle survival probabilities are plotted as a function of the tweezer separation, R_t . For the molecule we report the atom-pair survival probability, post-selected on cases where a weakly bound molecule was formed [55]. Upper panel: experimental runs where either a single Rb atom (blue squares) or a single RbCs molecule (red circles) is present. Lower panel: runs where both the atom and the molecule are present. The dashed lines (and shaded regions) correspond to the mean values (and errors) from the one-body cases. The purple dotted line at $R_t = 420$ nm shows the tweezer separation for the measurement in Fig. 4(a). Insets: The potential energy of the atom (blue) and molecule (red) resulting from their own tweezer (dashed lines) and both tweezers (solid lines) for $R_t = 2000$ (left) and $R_t = 420$ nm (right).

is present. The atomic survival probability is 97.2(4)%. For the molecule signal, we observe a survival probability of 48(2)%, primarily caused by loss prior to STIRAP due to the short lifetime of the state $|F\rangle$ in the trap. By compensating for the return STIRAP efficiency, we predict that a molecule in $|G\rangle$ is present in 53(3)% of runs in which a weakly bound molecule is created. The lower panel in Fig. 3 shows the two-body survival probabilities for runs in which *both* an atom and a weakly bound molecule are initially prepared. When the tweezers are brought together, the wave functions of the particles begin to overlap and collisions cause loss of both the molecule and atom. We observe a reduction in the atom survival probability by 58(6)%, commensurate with the probability a molecule in state $|G\rangle$ is present. From a Gaussian fit we find the loss falls to $1/e^2$ of its maximum value at $R_t = 250(20)$ nm.

To demonstrate blockade, we repeat the routine used to measure collisional loss, but use a shorter hold time of 3 μ s when the tweezers are close together. Two-photon excitation of the Rb atom $|g\rangle \rightarrow |6p_{3/2}\rangle \rightarrow |r\rangle$ is performed during the hold time with the trapping light still present [55]. Atoms excited to state $|r\rangle$ are antitrapped and ejected from the tweezers, mapping Rydberg excitation onto atom loss. To suppress collisional loss we hold the tweezers at a separation $R_t = 420(40)$ nm, shown by the dotted line in Fig. 3. Here the error represents the systematic

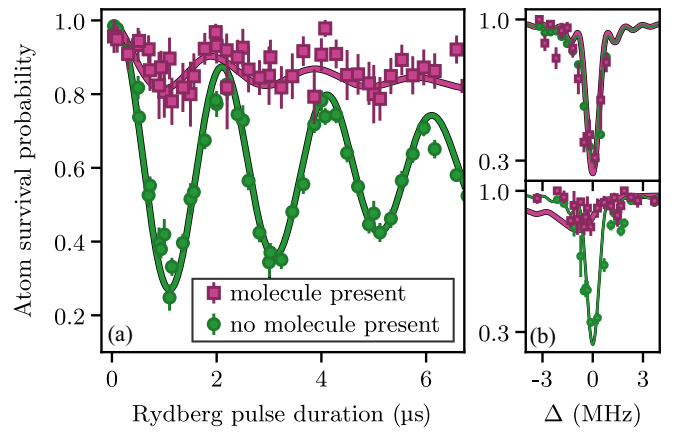


FIG. 4. (a) Survival probability of the Rb atom as a function of the Rydberg pulse duration for $R_{am} = 310(40)$ nm. Atoms excited to $|r\rangle$ are ejected from the trap and lost. Events are postselected on the detection of a molecule in $|G\rangle$ (purple squares) or unsuccessful formation of a molecule (green circles). The solid lines show the results of simulations using the Lindblad master equation [55] using our estimated atom-molecule separation. (b) Rb atom survival probability as a function of the two-photon detuning, Δ , using a 1 μ s pulse for $R_{am} = 700(40)$ nm (upper panel) and $R_{am} = 310(40)$ nm (lower panel). The detuning is defined relative to the transition center in the absence of a molecule. Symbols are as in (a) and solid lines show the results of simulations using the estimated atom-molecule separations.

uncertainty from the alignment calibrations. As shown inset in Fig. 3, this equates to an atom-molecule separation of $R_{am} = 310(40)$ nm [55].

In Fig. 4, we demonstrate the blockade of the Rydberg transition of the Rb atom when a RbCs molecule in state $|G\rangle$ is present. Figure 4(a) shows the survival probability of the Rb atom as the Rydberg pulse duration is varied. For experimental runs where the molecule tweezer is empty (green circles), we observe Rabi oscillations between states $|g\rangle$ and $|r\rangle$ with a fitted frequency of 500(3) kHz. The observed damping is caused by laser frequency noise. In contrast, for runs where a molecule in state $|G\rangle$ is present (purple squares), we observe a suppression of the excitation to state $|r\rangle$. Here, the presence of the molecule shifts the energy of state $|r\rangle$ through the charge-dipole interaction and thus blockades excitation during the Rydberg pulse. The frequency of the residual Rabi oscillations is almost identical to that for the unblocked case. This is due to the sharp onset of the interaction shown in Fig. 1(a) combined with shot-to-shot variations in the relative alignment of the tweezers. For runs with the largest separations, the energy shift is smaller than the Rabi frequency of the Rydberg transition leading to a signal at the unshifted Rabi frequency.

To simulate the expected excitation dynamics, we solve the Lindblad master equation [55]. We use the pair-state energy shifts shown in Fig. 1(a) to include a distance-dependent energy shift. We account for the fact that the atom and molecule are predominantly prepared in the

motional ground state of their respective tweezers by averaging the interaction over the ground-state wave function of relative motion. We also include experimental imperfections such as dephasing from laser frequency noise and shot-to-shot fluctuations in the relative alignment of the tweezers. Using our best estimates of the separation, we find good agreement between the results of the simulation and the experiment, as shown by the solid lines in Fig. 4(a).

Figure 4(b) shows the effect of changing the atom-molecule separation on the Rydberg blockade. In this experiment, we fix the pulse duration to approximate a π pulse and scan the two-photon detuning of the light driving the Rydberg transition. For $R_{\text{am}} = 700(40)$ nm, shown in the upper panel, the charge-dipole interaction is negligible. Here, the dominant interaction is van der Waals leading to a shift of ~ 0.1 kHz [86]. Consequently, the presence of a molecule does not affect the Rydberg excitation. However, for $R_{\text{am}} = 310(40)$ nm, shown in the lower panel, the presence of a molecule leads to an observed shift of the Rydberg transition to lower energy, as expected. The transition is significantly broadened due to the sensitivity of the charge-dipole interaction to the atom-molecule separation. The broadening causes a concomitant reduction in the signal amplitude. Both these effects are reproduced by simulations using the same parameters as in Fig. 4(a) with the exception of the appearance of a shoulder in the lower panel of Fig. 4(b) which is highly sensitive to fluctuations in R_{am} .

In conclusion, we have demonstrated blockade of the transition to the Rb(52s) Rydberg state due to the charge-dipole interaction with a RbCs molecule in the rovibrational ground state. This represents the first observation of a charge-dipole induced shift in an ultracold setting and opens up many new research directions. The blockade we have observed provides a mechanism for nondestructive state readout of the molecule [36,37]. A single Rydberg atom can also mediate effective spin-spin interactions between a pair of molecular dipoles [87]. For molecules prepared in the $N = 2$ rotational state, our calculations for the Rb(52s) Rydberg state predict that resolvable, deeply bound states exist for separations of ~ 220 nm. This offers the possibility to photoassociate giant polyatomic Rydberg molecules [46–48,88]. By selecting Rydberg and molecular states which interact via resonant dipole-dipole interactions, the Rydberg blockade radius can be increased to several microns, enabling high-fidelity entangling gates between molecules mediated by strong interactions with neighboring Rydberg atoms [38,39]. This presents the tantalizing prospect of a hybrid platform where quantum information is transferred between individually trapped molecules using Rydberg atoms.

The data presented in this Letter are available from [89].

We thank S. Spence for earlier experimental work, A. L. Tao for assistance in the setup of the STIRAP laser system,

X. Yang for informative simulations of the atom and molecule system, and H. J. Williams and S. A. Gardiner for helpful discussions. We acknowledge support from the UK Engineering and Physical Sciences Research Council (EPSRC) Grants EP/P01058X/1, EP/V047302/1, and EP/W00299X/1, UK Research and Innovation (UKRI) Frontier Research Grant EP/X023354/1, the Royal Society, and Durham University. R. G. F. gratefully acknowledges financial support by the Spanish projects PID2020–113390 GB-I00 (MICIN), PY20-00082 (Junta de Andalucía) and A-FQM-52-UGR20 (ERDF-University of Granada), and the Andalusian Research Group FQM-207. H. R. S. acknowledges support from the NSF through a grant for ITAMP at Harvard University.

A. G. and D. K. R. contributed equally to this work.

*c.s.adams@durham.ac.uk

†s.l.cornish@durham.ac.uk

- [1] R. Barnett, D. Petrov, M. Lukin, and E. Demler, Quantum Magnetism with Multicomponent Dipolar Molecules in an Optical Lattice, *Phys. Rev. Lett.* **96**, 190401 (2006).
- [2] A. V. Gorshkov, S. R. Manmana, G. Chen, J. Ye, E. Demler, M. D. Lukin, and A. M. Rey, Tunable Superfluidity and Quantum Magnetism with Ultracold Polar Molecules, *Phys. Rev. Lett.* **107**, 115301 (2011).
- [3] M. Baranov, M. Dalmonte, G. Pupillo, and P. Zoller, Condensed matter theory of dipolar quantum gases, *Chem. Rev.* **112**, 5012 (2012).
- [4] W. Lechner and P. Zoller, From Classical to Quantum Glasses with Ultracold Polar Molecules, *Phys. Rev. Lett.* **111**, 185306 (2013).
- [5] M. L. Wall, K. R. A. Hazzard, and A. M. Rey, Quantum magnetism with ultracold molecules, in *From Atomic to Mesoscale* (World Scientific, Singapore, 2015), Chap. 1, pp. 3–37.
- [6] J. L. Bohn, A. M. Rey, and J. Ye, Cold molecules: Progress in quantum engineering of chemistry and quantum matter, *Science* **357**, 1002 (2017).
- [7] N. Y. Yao, M. P. Zaletel, D. M. Stamper-Kurn, and A. Vishwanath, A quantum dipolar spin liquid, *Nat. Phys.* **14**, 405 (2018).
- [8] L. D. Carr, D. DeMille, R. V. Krems, and J. Ye, Cold and ultracold molecules: Science, technology and applications, *New J. Phys.* **11**, 055049 (2009).
- [9] M. Saffman, Quantum computing with atomic qubits and Rydberg interactions: Progress and challenges, *J. Phys. B* **49**, 202001 (2016).
- [10] C. S. Adams, J. D. Pritchard, and J. P. Shaffer, Rydberg atom quantum technologies, *J. Phys. B* **53**, 012002 (2019).
- [11] A. Browaeys and T. Lahaye, Many-body physics with individually controlled Rydberg atoms, *Nat. Phys.* **16**, 132 (2020).
- [12] M. Morgado and S. Whitlock, Quantum simulation and computing with Rydberg-interacting qubits, *AVS Quantum Sci.* **3**, 023501 (2021).
- [13] X. Wu, X. Liang, Y. Tian, F. Yang, C. Chen, Y.-C. Liu, M. K. Tey, and L. You, A concise review of Rydberg atom

- based quantum computation and quantum simulation, *Chin. Phys. B* **30**, 020305 (2021).
- [14] A. M. Kaufman and K.-K. Ni, Quantum science with optical tweezer arrays of ultracold atoms and molecules, *Nat. Phys.* **17**, 1324 (2021).
- [15] D. Jaksch, J. I. Cirac, P. Zoller, S. L. Rolston, R. Côté, and M. D. Lukin, Fast Quantum Gates for Neutral Atoms, *Phys. Rev. Lett.* **85**, 2208 (2000).
- [16] M. D. Lukin, M. Fleischhauer, R. Côté, L. M. Duan, D. Jaksch, J. I. Cirac, and P. Zoller, Dipole Blockade and Quantum Information Processing in Mesoscopic Atomic Ensembles, *Phys. Rev. Lett.* **87**, 037901 (2001).
- [17] L. Isenhower, E. Urban, X. L. Zhang, A. T. Gill, T. Henage, T. A. Johnson, T. G. Walker, and M. Saffman, Demonstration of a Neutral Atom Controlled-NOT Quantum Gate, *Phys. Rev. Lett.* **104**, 010503 (2010).
- [18] T. Wilk, A. Gaëtan, C. Evellin, J. Wolters, Y. Miroshnychenko, P. Grangier, and A. Browaeys, Entanglement of Two Individual Neutral Atoms Using Rydberg Blockade, *Phys. Rev. Lett.* **104**, 010502 (2010).
- [19] M. Saffman, T. G. Walker, and K. Mølmer, Quantum information with Rydberg atoms, *Rev. Mod. Phys.* **82**, 2313 (2010).
- [20] H. Levine, A. Keesling, G. Semeghini, A. Omran, T. T. Wang, S. Ebadi, H. Bernien, M. Greiner, V. Vuletić, H. Pichler, and M. D. Lukin, Parallel Implementation of High-Fidelity Multiqubit Gates with Neutral Atoms, *Phys. Rev. Lett.* **123**, 170503 (2019).
- [21] J. W. Park, Z. Z. Yan, H. Loh, S. A. Will, and M. W. Zwierlein, Second-scale nuclear spin coherence time of ultracold $^{23}\text{Na}^{40}\text{K}$ molecules, *Science* **357**, 372 (2017).
- [22] P. D. Gregory, J. A. Blackmore, S. L. Bromley, J. M. Hutson, and S. L. Cornish, Robust storage qubits in ultracold polar molecules, *Nat. Phys.* **17**, 1149 (2021).
- [23] S. Burchesky, L. Anderegg, Y. Bao, S. S. Yu, E. Chae, W. Ketterle, K.-K. Ni, and J. M. Doyle, Rotational Coherence Times of Polar Molecules in Optical Tweezers, *Phys. Rev. Lett.* **127**, 123202 (2021).
- [24] D. DeMille, Quantum Computation with Trapped Polar Molecules, *Phys. Rev. Lett.* **88**, 067901 (2002).
- [25] S. F. Yelin, K. Kirby, and R. Côté, Schemes for robust quantum computation with polar molecules, *Phys. Rev. A* **74**, 050301(R) (2006).
- [26] K.-K. Ni, T. Rosenband, and D. D. Grimes, Dipolar exchange quantum logic gate with polar molecules, *Chem. Sci.* **9**, 6830 (2018).
- [27] M. Hughes, M. D. Frye, R. Sawant, G. Bhole, J. A. Jones, S. L. Cornish, M. R. Tarbutt, J. M. Hutson, D. Jaksch, and J. Mur-Petit, Robust entangling gate for polar molecules using magnetic and microwave fields, *Phys. Rev. A* **101**, 062308 (2020).
- [28] R. Sawant, J. A. Blackmore, P. D. Gregory, J. Mur-Petit, D. Jaksch, J. Aldegunde, J. M. Hutson, M. R. Tarbutt, and S. L. Cornish, Ultracold polar molecules as qubits, *New J. Phys.* **22**, 013027 (2020).
- [29] V. V. Albert, J. P. Covey, and J. Preskill, Robust Encoding of a Qubit in a Molecule, *Phys. Rev. X* **10**, 031050 (2020).
- [30] L. R. Liu, J. D. Hood, Y. Yu, J. T. Zhang, N. R. Hutzler, T. Rosenband, and K.-K. Ni, Building one molecule from a reservoir of two atoms, *Science* **360**, 900 (2018).
- [31] L. Anderegg, L. W. Cheuk, Y. Bao, S. Burchesky, W. Ketterle, K.-K. Ni, and J. M. Doyle, An optical tweezer array of ultracold molecules, *Science* **365**, 1156 (2019).
- [32] X. He, K. Wang, J. Zhuang, P. Xu, X. Gao, R. Guo, C. Sheng, M. Liu, J. Wang, J. Li, G. V. Shlyapnikov, and M. Zhan, Coherently forming a single molecule in an optical trap, *Science* **370**, 331 (2020).
- [33] W. B. Cairncross, J. T. Zhang, L. R. B. Picard, Y. Yu, K. Wang, and K.-K. Ni, Assembly of a Rovibrational Ground State Molecule in an Optical Tweezer, *Phys. Rev. Lett.* **126**, 123402 (2021).
- [34] J. T. Zhang, L. R. B. Picard, W. B. Cairncross, K. Wang, Y. Yu, F. Fang, and K.-K. Ni, An optical tweezer array of ground-state polar molecules, *Quantum Sci. Technol.* **7**, 035006 (2022).
- [35] D. K. Ruttley, A. Guttridge, S. Spence, R. C. Bird, C. R. L. Sueur, J. M. Hutson, and S. L. Cornish, Formation of ultracold molecules by merging optical tweezers, *arXiv:2302.07296*.
- [36] E. Kuznetsova, S. T. Rittenhouse, H. R. Sadeghpour, and S. F. Yelin, Rydberg atom mediated polar molecule interactions: A tool for molecular-state conditional quantum gates and individual addressability, *Phys. Chem. Chem. Phys.* **13**, 17115 (2011).
- [37] E. Kuznetsova, S. T. Rittenhouse, H. R. Sadeghpour, and S. F. Yelin, Rydberg-atom-mediated nondestructive readout of collective rotational states in polar-molecule arrays, *Phys. Rev. A* **94**, 032325 (2016).
- [38] K. Wang, C. P. Williams, L. R. B. Picard, N. Y. Yao, and K.-K. Ni, Enriching the quantum toolbox of ultracold molecules with Rydberg atoms, *PRX Quantum* **3**, 030339 (2022).
- [39] C. Zhang and M. R. Tarbutt, Quantum computation in a hybrid array of molecules and Rydberg atoms, *PRX Quantum* **3**, 030340 (2022).
- [40] T. M. Graham, M. Kwon, B. Grinkemeyer, Z. Marra, X. Jiang, M. T. Lichtman, Y. Sun, M. Ebert, and M. Saffman, Rydberg-Mediated Entanglement in a Two-Dimensional Neutral Atom Qubit Array, *Phys. Rev. Lett.* **123**, 230501 (2019).
- [41] F. Järisch and M. Zeppenfeld, State resolved investigation of Förster resonant energy transfer in collisions between polar molecules and Rydberg atoms, *New J. Phys.* **20**, 113044 (2018).
- [42] K. Gawlas and S. D. Hogan, Rydberg-state-resolved resonant energy transfer in cold electric-field-controlled intrabeam collisions of NH_3 with Rydberg He atoms, *J. Phys. Chem. Lett.* **11**, 83 (2020).
- [43] S. Patsch, M. Zeppenfeld, and C. P. Koch, Rydberg atom-enabled spectroscopy of polar molecules via Förster resonance energy transfer, *J. Phys. Chem. Lett.* **13**, 10728 (2022).
- [44] B. Zhao, A. W. Glaetzle, G. Pupillo, and P. Zoller, Atomic Rydberg Reservoirs for Polar Molecules, *Phys. Rev. Lett.* **108**, 193007 (2012).
- [45] S. D. Huber and H. P. Büchler, Dipole-Interaction-Mediated Laser Cooling of Polar Molecules to Ultracold Temperatures, *Phys. Rev. Lett.* **108**, 193006 (2012).
- [46] S. T. Rittenhouse and H. R. Sadeghpour, Ultracold Giant Polyatomic Rydberg Molecules: Coherent Control of Molecular Orientation, *Phys. Rev. Lett.* **104**, 243002 (2010).

- [47] S. T. Rittenhouse, M. Mayle, P. Schmelcher, and H. R. Sadeghpour, Ultralong-range polyatomic Rydberg molecules formed by a polar perturber, *J. Phys. B* **44**, 184005 (2011).
- [48] R. González-Férez, S. T. Rittenhouse, P. Schmelcher, and H. R. Sadeghpour, A protocol to realize triatomic ultralong range Rydberg molecules in an ultracold KRb gas, *J. Phys. B* **53**, 074002 (2020).
- [49] B. Yan, S. A. Moses, B. Gadway, J. P. Covey, K. R. A. Hazzard, A. M. Rey, D. S. Jin, and J. Ye, Observation of dipolar spin-exchange interactions with lattice-confined polar molecules, *Nature (London)* **501**, 521 (2013).
- [50] L. Christakis, J. S. Rosenberg, R. Raj, S. Chi, A. Morningstar, D. A. Huse, Z. Z. Yan, and W. S. Bakr, Probing site-resolved correlations in a spin system of ultracold molecules, *Nature (London)* **614**, 64 (2023).
- [51] C. M. Holland, Y. Lu, and L. W. Cheuk, On-demand entanglement of molecules in a reconfigurable optical tweezer array, [arXiv:2210.06309](https://arxiv.org/abs/2210.06309).
- [52] Y. Bao, S. S. Yu, L. Anderegg, E. Chae, W. Ketterle, K.-K. Ni, and J. M. Doyle, Dipolar spin-exchange and entanglement between molecules in an optical tweezer array, [arXiv:2211.09780](https://arxiv.org/abs/2211.09780).
- [53] J. P. Shaffer, S. T. Rittenhouse, and H. R. Sadeghpour, Ultracold Rydberg molecules, *Nat. Commun.* **9**, 1965 (2018).
- [54] H. R. Sadeghpour, Ultracold Rydberg atom–atom interaction, in *Springer Handbook of Atomic, Molecular, and Optical Physics*, edited by G. W. F. Drake (Springer International Publishing, Cham, 2023), pp. 795–803.
- [55] See Supplemental Material at <http://link.aps.org/supplemental/10.1103/PhysRevLett.131.013401> for details of the theoretical calculations, STIRAP transfer, trap lifetimes, postselection scheme, and Rydberg excitation scheme. Supplemental Material includes Refs. [56–66].
- [56] A. Omont, On the theory of collisions of atoms in Rydberg states with neutral particles, *J. Phys. France* **38**, 1343 (1977).
- [57] U. Fano and A. Rau, 4—elastic scattering by a short-range central potential, in *Atomic Collisions and Spectra*, edited by U. Fano and A. Rau (Academic Press, New York, 1986), pp. 61–80.
- [58] J. Eaton, H. Sarkas, S. Arnold, K. McHugh, and K. Bowen, Negative ion photoelectron spectroscopy of the heteronuclear alkali-metal dimer and trimer anions: NaK^- , KRb^- , RbCs^- , KCs^- , Na_2K^- , and K_2Cs^- , *Chem. Phys. Lett.* **193**, 141 (1992).
- [59] M. Marinescu, H. R. Sadeghpour, and A. Dalgarno, Dispersion coefficients for alkali-metal dimers, *Phys. Rev. A* **49**, 982 (1994).
- [60] E. D. Black, An introduction to Pound–Drever–Hall laser frequency stabilization, *Am. J. Phys.* **69**, 79 (2001).
- [61] S. Weber, C. Tresp, H. Menke, A. Urvoy, O. Firstenberg, H. P. Büchler, and S. Hofferberth, Calculation of Rydberg interaction potentials, *J. Phys. B* **50**, 133001 (2017).
- [62] N. Šibalić, J. D. Pritchard, C. S. Adams, and K. J. Weatherill, ARC: An open-source library for calculating properties of alkali Rydberg atoms, *Comput. Phys. Commun.* **220**, 319 (2017).
- [63] S. de Léséleuc, D. Barredo, V. Lienhard, A. Browaeys, and T. Lahaye, Analysis of imperfections in the coherent optical excitation of single atoms to Rydberg states, *Phys. Rev. A* **97**, 053803 (2018).
- [64] H. Levine, A. Keesling, A. Omran, H. Bernien, S. Schwartz, A. S. Zibrov, M. Endres, M. Greiner, V. Vuletić, and M. D. Lukin, High-Fidelity Control and Entanglement of Rydberg-Atom Qubits, *Phys. Rev. Lett.* **121**, 123603 (2018).
- [65] J. T. Zhang, Y. Yu, W. B. Cairncross, K. Wang, L. R. B. Picard, J. D. Hood, Y.-W. Lin, J. M. Hutson, and K.-K. Ni, Forming a Single Molecule by Magnetoassociation in an Optical Tweezer, *Phys. Rev. Lett.* **124**, 253401 (2020).
- [66] J. A. Blackmore, R. Sawant, P. D. Gregory, S. L. Bromley, J. Aldegunde, J. M. Hutson, and S. L. Cornish, Controlling the ac Stark effect of RbCs with dc electric and magnetic fields, *Phys. Rev. A* **102**, 053316 (2020).
- [67] E. Fermi and E. Teller, The capture of negative mesotrons in matter, *Phys. Rev.* **72**, 399 (1947).
- [68] P. K. Molony, P. D. Gregory, Z. Ji, B. Lu, M. P. Köppinger, C. R. Le Sueur, C. L. Blackley, J. M. Hutson, and S. L. Cornish, Creation of Ultracold $^{87}\text{Rb}^{133}\text{Cs}$ Molecules in the Rovibrational Ground State, *Phys. Rev. Lett.* **113**, 255301 (2014).
- [69] P. D. Gregory, J. Aldegunde, J. M. Hutson, and S. L. Cornish, Controlling the rotational and hyperfine state of ultracold $^{87}\text{Rb}^{133}\text{Cs}$ molecules, *Phys. Rev. A* **94**, 041403(R) (2016).
- [70] R. V. Brooks, S. Spence, A. Guttridge, A. Alampounti, A. Rakonjac, L. A. McArd, J. M. Hutson, and S. L. Cornish, Preparation of one ^{87}Rb and one ^{133}Cs atom in a single optical tweezer, *New J. Phys.* **23**, 065002 (2021).
- [71] A. M. Kaufman, B. J. Lester, and C. A. Regal, Cooling a Single Atom in an Optical Tweezer to its Quantum Ground State, *Phys. Rev. X* **2**, 041014 (2012).
- [72] J. D. Thompson, T. G. Tiecke, A. S. Zibrov, and V. Vuletić, and M. D. Lukin, Coherence and Raman Sideband Cooling of a Single Atom in an Optical Tweezer, *Phys. Rev. Lett.* **110**, 133001 (2013).
- [73] S. Spence, R. V. Brooks, D. K. Ruttley, A. Guttridge, and S. L. Cornish, Preparation of ^{87}Rb and ^{87}Cs in the motional ground state of a single optical tweezer, *New J. Phys.* **24**, 103022 (2022).
- [74] K. Pilch, A. D. Lange, A. Prantner, G. Kerner, F. Ferlaino, H.-C. Nägerl, and R. Grimm, Observation of interspecies Feshbach resonances in an ultracold Rb-Cs mixture, *Phys. Rev. A* **79**, 042718 (2009).
- [75] T. Takekoshi, M. Debatin, R. Rameshan, F. Ferlaino, R. Grimm, H.-C. Nägerl, C. R. Le Sueur, J. M. Hutson, P. S. Julienne, S. Kotochigova, and E. Tiemann, Towards the production of ultracold ground-state RbCs molecules: Feshbach resonances, weakly bound states, and the coupled-channel model, *Phys. Rev. A* **85**, 032506 (2012).
- [76] M. P. Köppinger, D. J. McCarron, D. L. Jenkin, P. K. Molony, H.-W. Cho, S. L. Cornish, C. R. Le Sueur, C. L. Blackley, and J. M. Hutson, Production of optically trapped $^{87}\text{RbCs}$ Feshbach molecules, *Phys. Rev. A* **89**, 033604 (2014).
- [77] P. D. Gregory, P. K. Molony, M. P. Köppinger, A. Kumar, Z. Ji, B. Lu, A. L. Marchant, and S. L. Cornish, A simple,

- versatile laser system for the creation of ultracold ground state molecules, *New J. Phys.* **17**, 055006 (2015).
- [78] P. K. Molony, A. Kumar, P. D. Gregory, R. Kliese, T. Puppe, C. R. Le Sueur, J. Aldegunde, J. M. Hutson, and S. L. Cornish, Measurement of the binding energy of ultracold $^{87}\text{Rb}^{133}\text{Cs}$ molecules using an offset-free optical frequency comb, *Phys. Rev. A* **94**, 022507 (2016).
- [79] T. Takekoshi, L. Reichsöllner, A. Schindewolf, J. M. Hutson, C. R. Le Sueur, O. Dulieu, F. Ferlaino, R. Grimm, and H.-C. Nägerl, Ultracold Dense Samples of Dipolar RbCs Molecules in the Rovibrational and Hyperfine Ground State, *Phys. Rev. Lett.* **113**, 205301 (2014).
- [80] K. Bergmann, H. Theuer, and B. Shore, Coherent population transfer among quantum states of atoms and molecules, *Rev. Mod. Phys.* **70**, 1003 (1998).
- [81] N. V. Vitanov, A. A. Rangelov, B. W. Shore, and K. Bergmann, Stimulated Raman adiabatic passage in physics, chemistry, and beyond, *Rev. Mod. Phys.* **89**, 015006 (2017).
- [82] P. K. Molony, P. D. Gregory, A. Kumar, C. R. Le Sueur, J. M. Hutson, and S. L. Cornish, Production of ultracold $^{87}\text{Rb}^{133}\text{Cs}$ in the absolute ground state: Complete characterisation of the STIRAP transfer, *Chem. Phys. Chem.* **17**, 3811 (2016).
- [83] P. D. Gregory, J. A. Blackmore, F. M. D. L. M. Fernley, S. L. Bromley, J. M. Hutson, and S. L. Cornish, Molecule-molecule and atom-molecule collisions with ultracold RbCs molecules, *New J. Phys.* **23**, 125004 (2021).
- [84] P. Barakhshan, A. Marrs, A. Bhosale, B. Arora, R. Eigenmann, and M. S. Safronova, Portal for high-precision atomic data and computation (version 2.0), [Online] (2022), <https://www.udel.edu/atom/>.
- [85] R. Vexiau, D. Borsalino, M. Lepers, A. Orbán, M. Aymar, O. Dulieu, and N. Bouloufa-Maafa, Dynamic dipole polarizabilities of heteronuclear alkali dimers: Optical response, trapping and control of ultracold molecules, *Int. Rev. Phys. Chem.* **36**, 709 (2017).
- [86] V. Olaya, J. Pérez-Ríos, and F. Herrera, C_6 coefficients for interacting Rydberg atoms and alkali-metal dimers, *Phys. Rev. A* **101**, 032705 (2020).
- [87] E. Kuznetsova, S. T. Rittenhouse, I. I. Beterov, M. O. Scully, S. F. Yelin, and H. R. Sadeghpour, Effective spin-spin interactions in bilayers of Rydberg atoms and polar molecules, *Phys. Rev. A* **98**, 043609 (2018).
- [88] R. González-Férez, H. R. Sadeghpour, and P. Schmelcher, Rotational hybridization, and control of alignment and orientation in triatomic ultralong-range Rydberg molecules, *New J. Phys.* **17**, 013021 (2015).
- [89] A. Guttridge, D. K. Ruttley, A. C. Baldock, R. González-Férez, H. R. Sadeghpour, C. S. Adams, and S. L. Cornish, Observation of Rydberg blockade due to the charge-dipole interaction between an atom and a polar molecule [dataset] (Durham University), [10.15128/r2fj236215f](https://doi.org/10.15128/r2fj236215f).